

Bond Strength Evaluation of Waterproofing Membrane Assembly in Concrete Bridges

Yahia A. S. Khalayleh ¹, Aya Al-Asi ^{2*}, Ibrahim Asi ³, Roaa Alawadi ²

¹ Civil Engineering Department, The Hashemite University, Zarqa 13133, Jordan.

² Civil Engineering Department, Applied Science Private University, P.O. Box 166, Amman 11931, Jordan.

³ Civil Engineering Department, Al Ahliyya Amman University, Amman 19328, Jordan.

Received 07 December 2024; Revised 19 January 2025; Accepted 26 January 2025; Published 01 February 2025

Abstract

On the concrete bridge decks overlaid by HMA, slippage cracks usually appear on the HMA layer because of the presence of waterproofing membranes below the HMA layer and a lack of bonding of the membrane with the PCC underlying layer. The objective of this work is to develop a laboratory-based method for the fabrication of test samples of an HMA layer, waterproofing membrane, and PCC layer system. In addition, a bond strength test procedure was adapted to evaluate the bonding of the three layers assembly at different test temperatures in the laboratory prior to the field application. According to the obtained evaluation results, it was found that the weakest bond in the HMA, waterproofing membrane, and PCC assembly is the bond between the HMA layer and the waterproofing membrane. The bond strength of the assembly is highly affected by increasing temperature, since it lost approximately 75% of its strength when the test temperature increased from 25°C to 50°C. Likewise, as the test temperature increased from 25°C to 60°C, the assembly lost approximately 75% of its strength. Therefore, the bond strength should be evaluated at the expected pavement temperature in the field, specifically at the membrane interface level.

Keywords: HMA; PCC; Waterproofing Membrane; Bridge Construction; Pull-off Test; Bond Strength.

1. Introduction

In the construction of concrete bridges, water-impermeable membranes are placed on top of the Portland Cement Concrete (PCC) layer to protect the concrete reinforcement from water ingress; then, a hot mix asphalt (HMA) layer is placed on top of the membrane [1]. Many pavement failures occur due to poor bonding between the HMA layer and the waterproof membrane or between the waterproof membrane and the PCC underlying layer. The most frequently observed failure is slippage cracking and upheaval, which often occurs in locations where traffic experiences changes in speed (acceleration, deceleration) or at traffic turns, which affects driving comfort and reduces the service life of the bridge [2-4]. Imperfect bonding at the interfaces between the three layers results in high horizontal stresses and insufficient adhesion bonds between the pavement layers. Compaction difficulty, top-down cracking, premature fatigue, and surface delamination are also failures related to a lack of bonding between the layers [5, 6]. One common issue is slippage cracking because of weak bonding, which often occurs at intersections and near traffic lights, resulting in a significant decrease in the pavement's shear strength [7-9]. When there is weak bonding, water can penetrate through the pavement, and the asphalt layers do not function as a unified structure [10].

* Corresponding author: a_alaasi@asu.edu.jo

<http://dx.doi.org/10.28991/CEJ-2025-011-02-010>



© 2025 by the authors. Licensee C.E.J, Tehran, Iran. This article is an open access article distributed under the terms and conditions of the Creative Commons Attribution (CC-BY) license (<http://creativecommons.org/licenses/by/4.0/>).

Wang et al. reported that under moving loads, the transverse shear stress exceeds the longitudinal shear stress; additionally, the shear stress increases as the vehicle speed decreases [11]. To increase shear stress, polyurethane pavement materials were used as waterproof adhesive layers, but this led to a decrease in shear stress with an increasing amount of coating material [12]. Additionally, increasing the temperature with vehicle speed and horizontal load decreases the shear strength [13]. Many researchers have extensively studied several reasons for poor bonding between pavement layers. These reasons can be summarized as follows: type of tack coat, tack coat application rate, curing time, application temperature, asphalt residue content, pavement surface characteristics, asphalt cement content, type of aggregate, aggregate gradation, surface texture, surface cleanliness (method of cleaning the original surface), and environmental conditions [14, 15]. The bonding linking Portland cement concrete (PCC) pavement and hot-mix asphalt (HMA) surface layer is one of the most recognized and vital performance aspects tested in the design and construction of pavements [16]. Several investigations have concluded that having a poor bond strength at the interface between two materials leads to greater bending and shear stresses and deflection in composite pavement, resulting in abrupt pavement distress [17, 18]. In the most unfavorable cases, slippage cracks, severe rutting, or delamination may occur [19].

Flexible pavements are commonly used for their unique features, benefits, and adaptability. The top layer is usually the HMA layer, and the majority of flexible pavements consist of multiple layers of HMA or an HMA layer on top of a PCC concrete layer. These layers are connected via a tack coat so that the pavement layers behave as monolithic structures [20]. A tack coat is a light coating layer of bituminous binder. The main purpose of a tack coat is to create an adhesive surface between two asphalt layers in a new construction, between the old asphalt layer and the overlay layer during maintenance, or between the PCC layer and the top HMA layer. Tack coats also play a role in patching asphalt concrete pavements. They improve waterproofing in the asphalt layers and protect structural layers [21]. Tack coatings are sometimes referred to as bond coatings, especially when the adhesion strength between two layers is essential. A tack coat spray system is usually used to apply the tack coat. The hot asphalt mixture laid over the tack coat layer softens it, allowing it to cover surface voids in the new hot mix layer and promote bonding between the two layers [22]. In most of the available specifications for waterproofing membranes for concrete bridge decks, the specifications are only for the bond tensile strength within the membrane and the underlying PCC layer, and there are no specifications for the bond strength between the top HMA layer and the membrane. In addition, in these standards, the bond strength is specified at a maximum test temperature of 40°C, whereas the pavement temperature at the bonding interfaces might reach temperatures higher than 40°C [23].

The main aim of this research study is to develop a test procedure for laboratory and field evaluations of the bond strength between the hot mix asphalt layer, the interlayer membrane, and the bridge deck concrete layer at different test temperatures. In composite pavements, the bond strength between the HMA overlay and the PCC layer is affected by many factors, such as the type of mixture, PCC surface texture, tack coat, spreading rate of the tack coat, normal stress at the interface, and temperature. According to a study by Haido et al. [24], the splitting strength, compressive and flexural strengths, elasticity modulus, and Poisson's ratio at temperatures between 25°C and 50°C reduce the compressive and tensile strengths of self-compacting concrete by more than 20%.

A waterproof adhesive layer serves as a protective and structural layer between the bridge slab and the paving layer, confirming the consistency of the paving structure. Gao et al. [25] researched waterproof bonding materials and revealed that solvent-based asphalt waterproof bonding systems, epoxy asphalt, and waterborne epoxy-emulsified asphalt perform well at high temperatures. Therefore, it is essential to consider the shear performance of the waterproof-adhesive layer when designing bridge deck pavements. It also acts as a bonding and waterproofing agent, absorbs stress, inhibits surface cracking, and provides other benefits, such as resisting the hydrostatic pressure exerted by moisture in the liquid state [26, 27]. Many countries have adopted standards for the bond strength of waterproofing and the concrete layer at bridge decks. For example, Ireland [28] adopted the TII, and the United Kingdom adopted the BBA-HAPAS [29]. Similarly, the United States of America follows the NCHRP 425 standard for bond strength [30]. As shown in Figure 1, pull-off tests are recommended by all of the aforementioned standards to evaluate the failure stress between the waterproof membrane and the concrete layer.

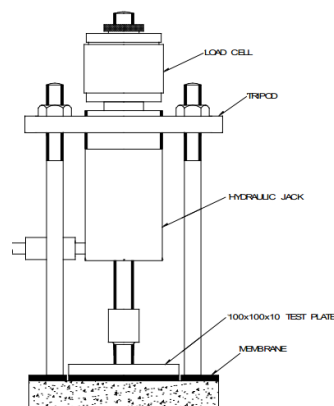


Figure 1. Example of a tensile pull-off, British Board of Agreements [29]

However, there are no specific tests or specification limits for the failure stress between the membrane and the asphalt layer, which is the weakest part in the structure. In addition, the International Specification Limits specify the bond strength at -10°C , 23°C and 40°C , whereas in many Middle Eastern countries, the pavement temperature at the waterproofing-HMA interlayer reaches 50°C . This study recommends a laboratory test procedure for evaluating the failure stress between the waterproof membrane and the asphalt layer or for evaluating the bond stress for the HMA layer, waterproof membrane, and PCC layer assembly. The suggested test procedure simulates the construction of the HMA layer on top of the membrane via a method that simulates and reproduces the real compaction conditions under actual road paving operations, including mix properties, compaction effort, and compaction temperature. The suggested test procedure also enables the evaluation of the bond strength of the structure assembly at different temperatures.

2. Experimental Program

To assess the bond strength of the HMA layer, membrane, and PCC layer assembly; twenty-four samples were fabricated via two types of waterproofing membranes, coarse and smooth surface membranes. The fabricated samples consisted of 15 cm diameter by 15 cm height PCC cylinders; waterproofing membranes were installed on top of the PCC cylinders, and then the PCC cylinder membrane assemblies were overlaid with 5 cm thick HMA layers. The HMA layers were compacted via the Superpave Gyrotory Compactor (SGC). SGC is considered the best HMA compaction equipment for simulating HMA field compaction [31, 32]. Fabricated samples were subjected to pull-off testing to evaluate the bond strength of the assembly at different testing temperatures (25°C , 40°C , 50°C , and 60°C). Figure 2 shows a schematic representation of the following experimental program.

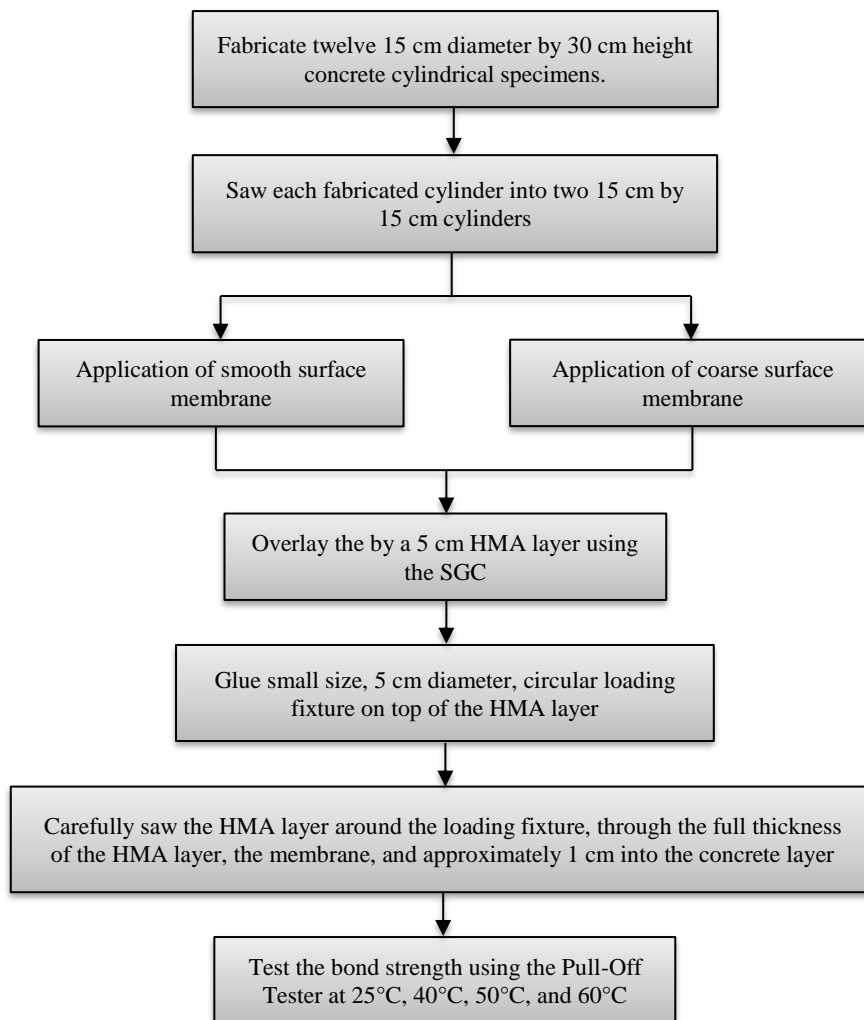


Figure 2. Experimental program

3. Materials and Fabrication of Test Samples

3.1. Concrete Mixture

The design of the concrete mixture was intended to produce a concrete strength of 25 MPa after 28 days. In addition to silica sand, it includes coarse, medium, and fine aggregates. The weights of the concrete mix design for one cubic meter are shown in Table 1. Concrete cylinders measuring 15 cm in diameter by 30 cm in height were cast, left to cure for 28 days, then were sawed into two 15 cm by 15 cm cylinders (Figure 3).

Table 1. Materials weights for one cubic meter of concrete

Material Type	Value
Coarse Agg.	332
Medium Agg.	617
Fine (Crushed Sand)	(kg/m ³) (Dry) 334
Silica Sand	620
Cement (OPC)*	(kg/m ³) 275
Water (Net)	162
Water (Total)	(lit/m ³) 176
W/C	0.59

* OPC: Ordinary Portland Cement



Figure 3. PCC sawed cylinders

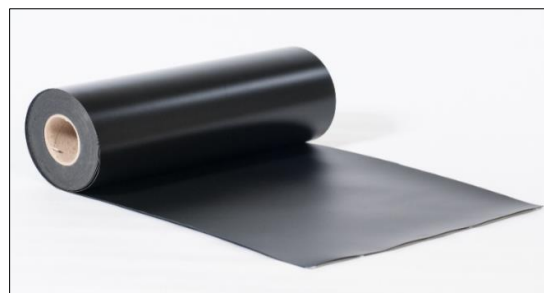
3.2. Waterproofing System

The waterproofing system consisted of three materials. First, a highly penetrative bituminous primer was applied on the concrete surface as the first layer. The primer used is a solvent-based, cold-applied, and highly penetrating thin bituminous solution with a black color. It is generally used for coating concrete surfaces, which should be clean and free of dust, dirt, oil, or humidity before application. Figure 4-a shows the applied primer layer.



(a)

(b)



(c)

Figure 4. Construction of the waterproof membrane, a) application of the primer layer on top of the concrete surface, b) application of the oxidized asphalt layer, and c) use of the waterproofing membrane

Next, tack coat was distributed at a specified rate of 0.3 kg/m² to promote better adhesion between the mastic asphalt and the concrete surface. The tack coat ensures a stronger bond between the layers. Following the tack coat, mastic asphalt was used at a rate of 40 kg/m². Then a mastic asphalt layer was applied on top of the tack coat. The mastic asphalt was produced by air-blowing petroleum waste products, which were subsequently mixed with silty sand, crushed limestone, cement, and hydrated lime. Mastic asphalt acts as an adhesive layer. Figure 4-b shows the application of the mastic asphalt layer.

In the last stage, a 5 mm thick waterproofing membrane (Figure 4-c) was laid on the mastic asphalt. The membrane is made of bitumen that has been modified with atactic polypropylene (APP). The compound is a mixture of distilled bitumen, thermoplastic polymers, and elastoplastic copolymer, which makes the membrane highly durable and flexible even at low temperatures and able to withstand high temperatures. The membrane was reinforced with 200 g/m² of nonwoven polyester fabric to achieve approximately 45–50% elongation and provide the membrane with the required resistance to heat aging, punching, and rutting. To avoid adhering to the roll and rapidly melting when heated during membrane installation, the membrane is made with a polyethylene coating on the underside. The properties of the utilized membrane are displayed in Table 2.

Table 2. Properties of the used waterproofing membrane

Property	Value	Test Method
Dimension, m/roll	1×10	-
Thickness, mm	5	ASTM D5147
Weight per roll, kg	62	UEAtc MOAT 30
Reinforcement	Nonwoven Polyester 200 g/m ²	-
Penetration of coating mixture at 25°C, DMM	20 ± 10	ASTM D5
Softening point of coating mixture, °C	150 ± 10	ASTM D36
Heat Resistance	No flowing after 2 hours at 120°C.	BS EN 1110
Cold Pliability	No cracking at -12°C	BSEN1109
Tensile Strength, N/5 cm		
Longitudinal	850	ASTM D5147, D146 and BSEN 12311
Transverse	650	
Water Absorption, %	<1	ASTM D5147
Water Pressure Resistance	No leakage at 1000 mm water head/24 hrs.	UEAtc MOAT 27
Water Vapor Transmission	0.2 g/m ² per day	ASTM E96
Resistance to Chemicals	Resistant to alcohol, salt solutions, dilute acids, and alkalis.	-

In this study, we developed two types of membranes: a smooth surface membrane and a coarse surface membrane. Both were used to evaluate their impact on the bond strength with the HMA and PCC layers. While shot blasting or milling is typically used in bridge construction to prepare the levelling layer, our study focused on the bond strength between the membrane and the HMA layer under monitored conditions. The smooth and coarse membranes simulate the surface conditions before such treatments, allowing the evaluation of the influence of membrane surface characteristics on bonding.

During membrane manufacturing, the upper face of the membrane can be left without coverage with other materials to have a smooth surface or can be covered with fine sand and fine granules to obtain a coarse surface. To fix the sheet to the lower layers, a propane gas burner is used to melt off the polyethylene film and to form a thin layer of melted bitumen while unrolling and laying the membrane.

In this research, two types of membranes were used, the smooth surface and the coarse surface. Twelve samples were fabricated with a smooth surface membrane, and twelve samples were fabricated with a coarse surface membrane. The fabricated samples were subjected to pull-off testing at four test temperatures (25°C, 40°C, 50°C, and 60°C). Three samples from each group were tested at each test temperature.

3.3. Asphalt Mixture

Table 3 presents the key performance properties and mix proportions of the asphalt HMA mixture. Bitumen, grade 60/70, produced from the Jordanian Petroleum Refinery was used in the HMA mixture. The asphalt mixture was designed to achieve HMA with air voids of 5.0%, ensuring both durability and structural integrity. The particle size distribution curve of the HMA mixture used is presented in Figure 5.

Table 3. Asphalt mixture proportions and properties

Performance Characteristic	Value	Unit
Bitumen Type	60/70	-
Bitumen Source	Jordanian Petroleum Refinery	-
bitumen content by weight of total mix	4.82	%
bitumen content by weight of aggregate	4.60	%
Unit weight at recommended bitumen content	2.439	gm/cm ³
Stability at Recommended bitumen content	1962	kN
Flow at recommended bitumen content	2.7	mm
Stiffness at recommended bitumen content	719	g/mm
Air voids at recommended bitumen content	5.0	%
VMA at recommended bitumen content	15.8	%
Loss of Stability	15.3	%
Filler/Bitumen Ratio	1.23	-
Air voids at refusal	2.1	%

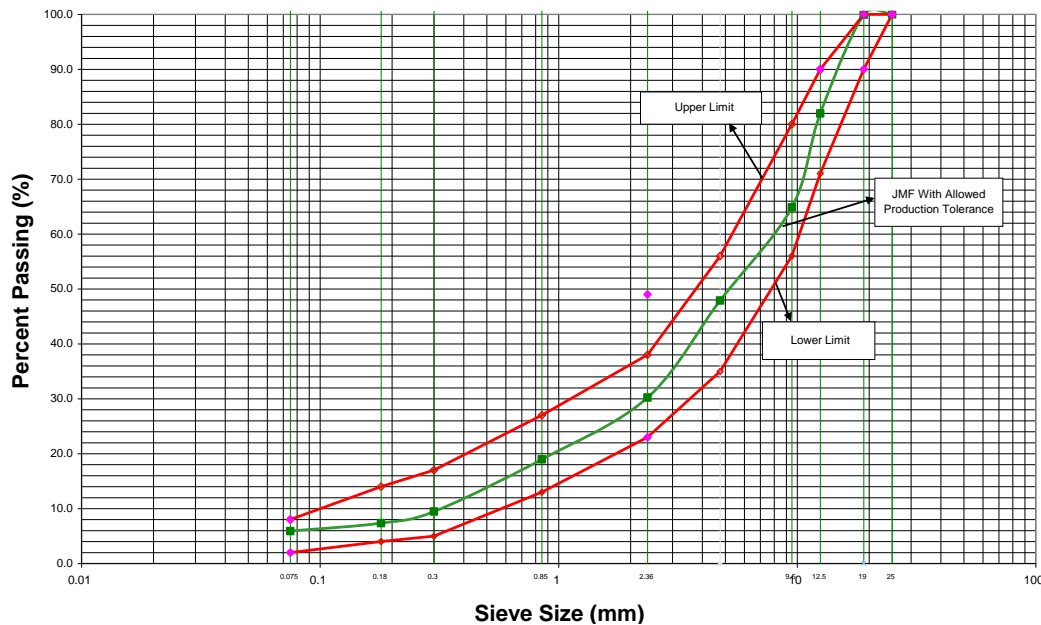


Figure 5. Particle size distribution curve of the aggregates used in HMA

3.4. Superpave Gyrotory Compactor

The Superpave Gyrotory Compactor (SGC) is a computer-controlled compaction device designed to accommodate large-size aggregates to reduce the effect of boundary conditions. It combines both the rotary compaction action and the vertical resultant force on the HMA. Extensive studies by Galaviz-González et al. [10], Shabani et al. [33], and Wang et al. [34] determined that the SGC is the most popular HMA compaction equipment that simulates field compaction. This represents the HMA compaction that occurs in the field during construction and eventual traffic loading.

The main parameters governing the compaction effort are the vertical pressure, 600 ± 18 kPa; the gyration angle of the mound, $1.16 \pm 0.02^\circ$ (internal), $1.25 \pm 0.02^\circ$ (external); the gyration rate, 30.0 ± 0.5 gyrations per minute; and the number of gyrations, which are based on the expected traffic level, or target air voids. The HMA mixtures were compacted using the SGC on top of the waterproofing membrane to achieve air void content of 5%. The HMA compaction temperature was maintained at 140°C to attain the proper HMA mix characteristics and the required bonding strength between the waterproofing membrane and the HMA layer.

3.4.1. Selection of the Specimen Thickness and Test Temperatures

Xu et al. [35] reported that the ambient temperature significantly influences the temperature within the top 5 cm of asphalt pavement. Furthermore, the study revealed that the bond strength was affected within the top 2–5 cm of the pavement depth. In addition, since the usual thickness of the HMA layer on top of the PCC layer on the HMA bridge decks is 5 cm, the selected thickness of the HMA layer was 5 cm.

The temperature of the asphalt layer also varies with depth from the top of the surface of the layer. Zhang et al. [36] developed a preventive technique for avoiding cracks in asphalt pavement. According to the developed equation, with a maximum air temperature of 50°C and a pavement depth of 5 cm, the pavement temperature is approximately 60°C. To measure the effectiveness of the pavement temperature on the bond strength between the waterproofing membrane and the asphalt layer and cover the upper temperature that the asphalt layer at a depth of 5 cm might reach, four test temperatures were selected: 25°C, 40°C, 50°C, and 60°C [36].

These results support the impact of the polypropylene geotextile retaining good deformability and strength with high thermal stability when interacting with thermal shocks at a temperature of 180°C. The recorded melting point was 166 °C, and the thermal decomposition point was 400 °C. The glass transition point was measured at a temperature between -20 and -10°C. The bridge's paving structure has a strong bond because the structure has not demonstrated any temperature sensitivity. Moreover, the mixture of asphalt was waterproof after drying. The results indicate that a pavement structure integrated with a composite stress-absorbing layer reduces cracking (CSAL), especially at lower temperatures. The technique is five times better than the circumstances in which preventive measures are not addressed and the project's security is not secured. Even at the 2 mm amplitude, the chances of forming reflective cracks on the structure were still slightly lower at a temperature of 20 °C than those of the asphalt rubber stress-absorbing membrane interlayer (ARSAMI). In all the deformation scenarios, CSAL outperformed ARSAMI in terms of structural and standing forms [36].

A sample height of 15 cm was chosen for practical reasons related to the available testing equipment and ease of handling. While the typical leveling layer in expressways is 10 cm, the extra 5 cm allowed for better sample stability and did not affect the primary focus of the bond strength testing, as the interaction between the HMA, membrane, and PCC layers was still adequately represented.

3.4.2. Pull-off Tensile Tests

The tension pull-off test is a standard method used to evaluate the pull-off strength of coatings on concrete via portable pull-off adhesion testers, ASTM D 7234. This test assesses the ultimate force required to pull the coating or material away from the substrate under tension. The test is usually performed via a tensile loading fixture that applies a controlled tensile force to a small circular loading fixture, with a flat surface on one end that can be adhered to the test surface/coating and a means of attachment to the tester on the other end. The loading fixture is glued to the substrate and left to dry. The pull-off tester is fixed to the attachment of the circular loading fixture, and the pull-off tensile load is gradually increased until the bond between the coating and the substrate fails, resulting in the coating detaching from the surface.

However, this study utilizes a testing system that differs from the British Board of Agreements standard, primarily in terms of sample size. The sample size selected for this research was adequate for obtaining reliable bond strength measurements. Despite the smaller sample size, it is still considered suitable for evaluating the bond strength between the HMA layer and the waterproofing membrane. The results were further validated by replicating the tests with multiple samples.

3.5. Test Procedure

Twenty-four test samples were fabricated, each consisting of a 15 cm diameter by 15 cm height concrete cylinder and waterproofing membrane, fixed according to the abovementioned procedure, overlaid with a 5 cm HMA layer, and compacted with the SGC to obtain 5% air voids (Figure 6). A smooth surface membrane was used for twelve of the test samples, and a coarse surface membrane was used for the other twelve test samples.



Figure 6. Prepared test samples

The test samples for each waterproofing membrane type were grouped into three replicate groups and tested at 25°C, 40°C, 50°C, and 60°C. Therefore, the test variables were the membrane surface type (smooth or coarse) and test temperature (25°C, 40°C, 50°C, or 60°C).

After the small size, 5 cm diameter, circular loading fixture on top of the HMA layer was glued and allowed sufficient time for it to dry, the HMA layer was carefully sawed around the fixture through the full thickness of the HMA layer, the membrane, and approximately 1 cm into the concrete layer, ensuring that the bond strength was not affected (Figure 7). The pull-off tester was fixed to the screwed attachment of the circular loading fixture (Figure 8), and the pull-off tensile load was gradually increased until the bond between the HMA layer and the substrate failed, resulting in detachment of the HMA layer from the PCC sample. The bond failure surface was recorded, either between the HMA layer and the membrane or between the membrane and the PCC layer. After the pull-off test, the failure surface area was measured in detail. This involved examining the failure zone on the central portion of the sawed test sample.



Figure 7. The circular loading fixture is glued to the top surface of the HMA layer



Figure 8. Pull-off test setup

Before the test samples were exposed to pull-off testing, they were preconditioned at the desired test temperature for a minimum of two hours. Both the failure surface and the failure pull-off load were recorded for each test sample. The pull-off strength was obtained by dividing the pull-off failure load by the area of the centerpiece of the sawed test sample.

4. Results and Discussion

Table 4 shows the bond strength results for both the surface membrane types and the tested samples at various test temperatures. Figure 9 shows the values for both membrane surface types.

Table 4. Pull-off test results

Specimen	Test temperature (°C)	Stress (MPa)			
		Sample 1	Sample 2	Sample 3	Average
Coarse Surface Membrane	25	0.622	0.596	0.612	0.610
	40	0.234	0.251	0.265	0.250
	50	0.143	0.142	0.135	0.140
	60	0.054	0.056	0.052	0.054
Smooth Surface Membrane	25	0.673	0.661	0.676	0.670
	40	0.252	0.278	0.280	0.270
	50	0.164	0.166	0.150	0.160
	60	0.087	0.099	0.102	0.096

A comparison of the pull-off test results for the coarse and smooth surface membranes clearly reveals that the failure stress decreases with increasing temperature. This finding indicates that the bond between asphalt and concrete weakens as the temperature increases.

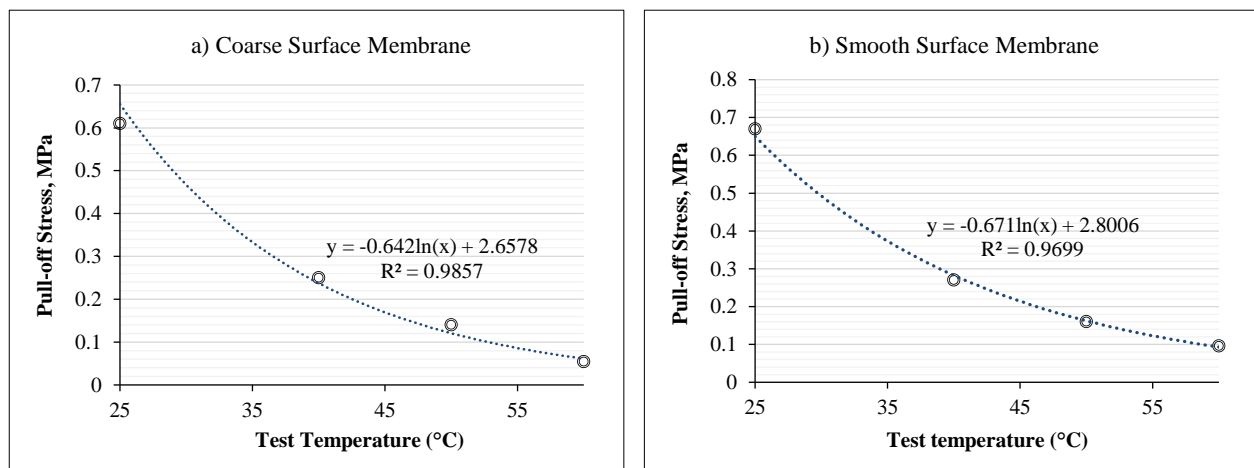


Figure 9. Pull-off bond strength for a) the coarse surface membrane and b) the smooth surface membrane

Regression analysis was used to determine the relationship between the obtained pull-off bond strength and the pavement temperature.

Two formulas were obtained for both types of membrane surfaces:

For a coarse surface membrane,

$$\text{Pull-Off Bond Strength (MPa)} = -0.642 \ln(\text{Pavement temperature}) + 2.6578 \text{ with } R^2 = 0.9841 \tag{1}$$

For a smooth surface membrane,

$$\text{Pull-Off Bond Strength (MPa)} = -0.671 \ln(\text{Pavement temperature}) + 2.8006 \text{ with } R^2 = 0.9685 \tag{2}$$

Figure 10 shows the average pull-off test results for both types of membrane surfaces. Figure 10 shows that at all test temperatures, the bond strength of the smooth surface membranes is greater than that of the coarse surface membranes, which might be attributed to the greater contact surface area of the smooth surface membranes than that of the coarse surface membranes.

For the coarse surface membrane, at 25°C, the average pull-off strength was 0.610 MPa, whereas at 50°C, it decreased to 0.140 MPa, and at 60°C, it decreased to 0.054 MPa. This indicates that the pull-off strength decreased by 77% and 91% when the temperature was raised from 25°C to 50°C and 60°C, respectively. Similarly, the pull-off strength decreased by 76% and 86% as the temperature was raised from 25°C to 50°C and 60°C, respectively. Therefore, the bond strength should be evaluated at the expected in situ pavement temperature since the bond strength is highly affected by temperature.

For all the tested samples, failure occurred at the interface between the asphalt layer and waterproofing membrane, resulting in a smooth, peel off, failure surface (Figure 11). This finding conflicts with the International Standards for waterproofing and surfacing of concrete bridge decks, since they specify a limit for the bond strength between the waterproofing membrane and the underlying bridge concrete layer and ignore the bond between the waterproofing membrane and the HMA layer. In addition, they specify the test limits at -10°C, 23°C, and 40°C and ignore the bond strength at higher temperatures, where the bond strength is more critical.

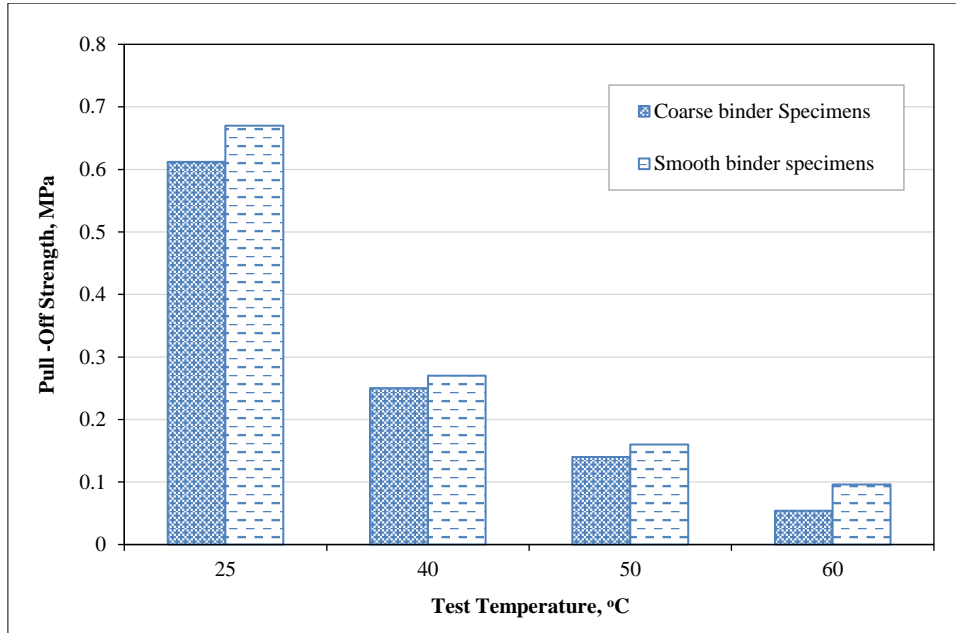


Figure 10. Average pull-off test results for the coarse and smooth surface membranes



Figure 11. Failure interface between the HMA layer and the waterproofing membrane

The shear bond strength of the HMA, membrane, and PCC layers can be assessed by fabricating test samples via the recommended sample preparation method and then testing their shear strength via a Leutner shear strength tester [37], layer-parallel direct shear (LPDS) testing device [38], NCAT bond strength device [39], or LCB shear test setup [40], as indicated in Figure 12.

In addition, the suggested pull-off test procedure can be used to assess the bond strength of the HMA layer, waterproofing membrane, and PCC lathe field. This can be accomplished by gluing a small, 5 cm diameter, circular loading fixture on top of the HMA layer and leaving it for enough time to dry. The assembly was then sawed around all sides in the tensile fixture, up to the full thickness of the HMA layer, through the membrane, and approximately one cm inside the concrete layer. Then, pull-off testing was performed. Coring cannot be used to core through the HMA layer since the torque exerted by the machine between the HMA layer and the membrane is greater than the bond strength between them. Therefore, the HMA layer separates from the membrane during the coring process.

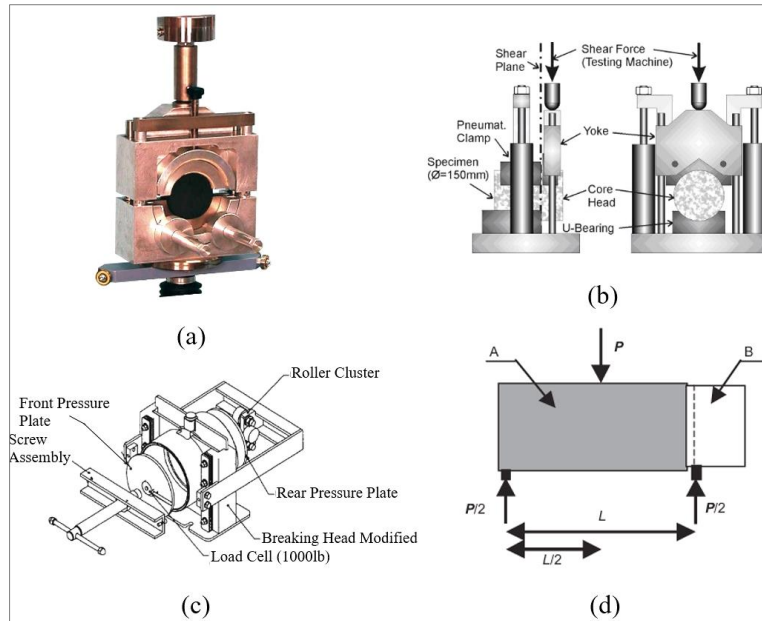


Figure 12. Shear Interlayer Bond Evaluation Test Devices; a) Leutner Shear Strength Tester, [37]; b) Layer-Parallel Direct Shear (LPDS) testing device [38]; c) NCAT Bond Strength Device [39]; d) LCB shear test setup [40]

4.1. Analysis of Variance (ANOVA)

The test data were collected and analyzed statistically to determine whether the pull-off bond strength is significantly affected by the membrane surface type and the test temperature. The analysis was performed via ANOVA for the single-factor model. ANOVA is used to test for significant differences between variables or treatment means. To test the equality of variable or treatment means, the following hypothesis is checked as a standard procedure [41]:

$$H_0: \mu_1 = \mu_2 = \mu_3 = \dots \mu_a \tag{3}$$

$$H_1: \mu_i \neq \mu_j \tag{4}$$

where μ_i represents the overall mean values for the various evaluated variables, which are the membrane surface type and test temperature. If H_0 is factual, the pull-off strength is not affected by these variables. However, if H_0 is not true, then there is a significant effect of the variable on the pull-off strength, and it is improbable that the variable means are equivalent. The ANOVA calculations were accomplished statistically via Microsoft Excel software. Statistically significant results are obtained when the calculated P-level is below the chosen significance level (SL), which is generally 5%. This indicates that for 95% SL, to achieve a considerable influence of any factor, the P-level should be less than 0.05, i.e., the P-level value illustrates a decreasing measure of the reliability of the result. In other words, the greater the P-level is, the less reliable the results are. Essentially, the P-level represents the probability of error that comes with taking the observed results as a valid estimate of the population. In the majority of analyses, a P-level of 0.05 is typically considered a "borderline for an appropriate" error level. The F statistic is another measure of significance testing that compares the variation caused by regression to the unexplained variability. This value should be greater than the F-critical value. Table 5 presents an overview of the ANOVA results for the impact of the test temperature on the pull-off strength.

Table 5. ANOVA results for the effect of temperature on the pull-off strength

ANOVA: Single Factor Analysis						
Groups (Temperature, °C)	Count	Sum	Average	Variance		
25	6	3.84	0.64	0.001174		
40	6	1.56	0.26	0.000314		
50	6	0.9	0.15	0.000158		
60	6	0.45	0.075	0.000556		
ANOVA						
Source of Variation	SS	df	MS	F	P value	F critical
Between Groups	1.133513	3	0.377838	686.3533	2.5E-20	3.098391
Within Groups	0.01101	20	0.000551			
Total	1.144523	23				

Table 5 shows that the mean square value (0.377838) between the different temperature groups is significantly higher than the within-temperature groups or mean square error (0.000551). This finding reveals that it is improbable that the pull-off strengths indicate that the different temperatures are equal. The F ratio can be determined (i.e., $F_0 = 0.377838/0.000551 = 686.3533$) and compared with $F_{critical} = 3.0984$. Since $F_0 > F_{critical}$, H_0 is rejected, and the means of the temperature groups are different, i.e., the test temperature dramatically affects the pull-off strength. This can be verified by the low P level ($2.5E-20 < 0.05$), indicating the strong effect of the test temperature.

A summary of the ANOVA results for the effect of the membrane surface type on the pull-off strength is presented in Table 6. Table 6 shows that the calculated F ratio for the effect of the membrane surface type on the pull-off strength is 0.146314, which is lower than $F_{critical} = 4.30095$. Since F_0 is not $> F_{critical}$, H_0 cannot be rejected, and it can be concluded that the membrane surface type group mean is not different, i.e., the membrane surface type does not significantly affect the pull-off strength. Therefore, although Figure 10 indicates that, at all test temperatures, the average values of the pull-off bond strength of the smooth surface membrane samples are greater than those of the coarse surface membrane samples are, the statistical analysis of the obtained results for all the test samples proved that the differences in the obtained pull-off strengths between the two evaluated types of surfaces are not significant. Therefore, the pull-off results for both types of surfaces can be grouped. Regression analysis to correlate the obtained pull-off bond strength with the pavement temperature was repeated by pooling the results of both membrane surface types. The developed regression formula for the pooled results, ignoring the effect of the membrane surface type, is as follows:

$$\text{Pull-Off Bond Strength (MPa)} = -0.657 \ln(\text{Pavement temperature}) + 2.7292 \text{ with } R^2 = 0.9690 \quad (5)$$

Table 6. ANOVA results for the effect of the membrane surface type on the pull-off strength

ANOVA: Single Factor Analysis						
Groups (Membrane Surface Type)	Count	Sum	Average	Variance		
coarse	12	3.162	0.2635	0.049003		
fine	12	3.588	0.299	0.054357		
ANOVA						
Source of Variation	SS	df	MS	F	P value	F critical
Between Groups	0.007562	1	0.007562	0.146314	0.705754	4.30095
Within Groups	1.136961	22	0.05168			
Total	1.144523	23				

5. Conclusions

In this study, a pull-off test was used to measure the bond strength between the HMA layer, waterproofing membrane, and PCC layer assembly. A Superpave gyratory compactor was used to compact the HMA layer to simulate the HMA field compaction density and compaction temperature. Bond strength testing was performed at various temperatures to assess how the temperature affected the bond strength of the HMA, membrane, and PCC assemblies.

Pull-off testing involves applying a tensile force to assess the bond strength of the HMA, membrane, and PCC assemblies. In this study, two groups of samples were fabricated; in the first group, a coarse surface membrane was used, while a smooth surface membrane was used in the second group. Both groups of samples were tested at different test temperatures (25°C, 40°C, 50°C, and 60°C).

The following observations can be concluded from the obtained test results:

- The developed sample preparation procedure and bond evaluation technique can be used to evaluate the strength of the bond between all the layers in the HMA layer, waterproofing membrane, and PCC layer assembly at the expected in situ field temperature at the membrane interface level.
- For all the tested samples, the failure of the bond was between the HMA layer and the membrane rather than between the membrane and the PCC layer. Therefore, efforts should be made to evaluate the bond strength of the entire assembly rather than concentrating on the bond between the membrane and the underlying PCC layer.
- The test temperature significantly affects the bond strength of the test assembly. Therefore, the bond strength should be evaluated at the expected pavement temperature in the field, specifically at the membrane interface level.
- Although the obtained test results did not prove the significant effect of the membrane surface type for the two types of surfaces evaluated in this study, the membrane surface type might have a considerable effect on the bond strength for other types of membranes or surface types.
- Test samples that can be assessed for both tensile and shear bond strength by testing equipment and setups that are currently available can be created via a developed sample preparation technique.
- The adopted testing procedure can be used to evaluate the bond strength of the HMA layer, waterproofing membrane, and PCC layer in the field.

6. Declarations

6.1. Author Contributions

Conceptualization, Y.A.S.K. and I.A.; methodology, A.A.A. and R.A.; validation, I.A., Y.A.S.K., and R.A.; formal analysis, A.A.A.; investigation, I.A. and Y.A.S.K.; resources, R.A.; data curation, A.A.A.; writing—original draft preparation, A.A.A. and R.A.; writing—review and editing, I.A. and Y.A.S.K.; visualization, Y.A.S.K.; supervision, I.A. All authors have read and agreed to the published version of the manuscript.

6.2. Data Availability Statement

The data presented in this study are available in the article.

6.3. Funding

The authors received no financial support for the research, authorship, and/or publication of this article.

6.4. Conflicts of Interest

The authors declare no conflict of interest.

7. References

- [1] Kokkalis, A., & Panetsos, P. (2015). Asphalt bridge deck pavement behavior, the Egnatia experience. *Bituminous Mixtures and Pavements*, 6, 789–793. doi:1201/b18538-112.
- [2] He, Q., Zhang, H., Li, J., & Duan, H. (2021). Performance evaluation of polyurethane/epoxy resin modified asphalt as adhesive layer material for steel-UHPC composite bridge deck pavements. *Construction and Building Materials*, 291, 123364. doi:10.1016/j.conbuildmat.2021.123364.
- [3] Nafaa, S., Ashour, K., Mohamed, R., Essam, H., Emad, D., Elhenawy, M., Ashqar, H. I., Hassan, A. A., & Alhadidi, T. I. (2024). Automated Pavement Cracks Detection and Classification Using Deep Learning. 2024 IEEE 3rd International Conference on Computing and Machine Intelligence (ICMI), 1–5. doi:10.1109/icmi60790.2024.10586098.
- [4] Kruntcheva, M. R., Collop, A. C., & Thom, N. H. (2005). Effect of bond condition on flexible pavement performance. *Journal of Transportation Engineering*, 131(11), 880–888. doi:10.1061/(ASCE)0733-947X(2005)131:11(880).
- [5] Al-Mansour, A., Zhu, Y., Lan, Y., Dang, N., Alwathaf, A. H., & Zeng, Q. (2024). Improving the adhesion between recycled plastic aggregates and the cement matrix. *Reuse of Plastic Waste in Eco-efficient Concrete*. Woodhead Publishing, Sawston, United Kingdom. doi:10.1016/B978-0-443-13798-3.00008-5.
- [6] West, R. C., Zhang, J., & Moore, J. (2005). Evaluation of bond strength between pavement layers (No. NCAT Report 05-08). National Center for Asphalt Technology, Auburn University, Auburn, United States.
- [7] Li, S., Zhang, L., Guo, P., Zhang, P., Wang, C., Sun, W., & Han, S. (2021). Characteristic analysis of acoustic emission monitoring parameters for crack propagation in UHPC-NC composite beam under bending test. *Construction and Building Materials*, 278, 122401. doi:10.1016/j.conbuildmat.2021.122401.
- [8] Somé, S. C., Feeser, A., Jaoua, M., & Le Corre, T. (2020). Mechanical characterization of asphalt mixes inter-layer bonding based on reptation theory. *Construction and Building Materials*, 242, 118063. doi:10.1016/j.conbuildmat.2020.118063.
- [9] Yang, K., & Li, R. (2021). Characterization of bonding property in asphalt pavement interlayer: A review. *Journal of Traffic and Transportation Engineering (English Edition)*, 8(3), 374–387. doi:10.1016/j.jtte.2020.10.005.
- [10] Galaviz-González, J. R., Cueva, D. A., Covarrubias, P. L., & Palacios, M. Z. (2019). Bonding evaluation of asphalt emulsions used as tack coats through shear testing. *Applied Sciences (Switzerland)*, 9(9), 1727. doi:10.3390/app9091727.
- [11] Wang, L., Hou, Y., Zhang, L., & Liu, G. (2017). A combined static-and-dynamics mechanics analysis on the bridge deck pavement. *Journal of Cleaner Production*, 166, 209–220. doi:10.1016/j.jclepro.2017.08.034.
- [12] Xu, Y., Fan, Z., Wang, Z., Shan, H., Lyu, X., Liu, Z., & Xu, S. (2024). Research on anti-shear performance of waterproof adhesive layer (WAL) in polyurethane-mixture steel-bridge pavement structure. *Construction and Building Materials*, 417, 135314. doi:10.1016/j.conbuildmat.2024.135314.
- [13] Lei, X., Li, T., & Chen, H. (2025). Mechanical analysis and experimental study on the shear performance of waterproof adhesive layer toward concrete bridge deck pavement. *Case Studies in Construction Materials*, 22, e04250. doi:10.1016/j.cscm.2025.e04250.
- [14] Rahman, A., Huang, H., Ai, C., Ding, H., Xin, C., & Lu, Y. (2019). Fatigue performance of interface bonding between asphalt

- pavement layers using four-point shear test set-up. *International Journal of Fatigue*, 121, 181–190. doi:10.1016/j.ijfatigue.2018.12.018.
- [15] Zhang, Q., Xu, Y. H., & Wen, Z. G. (2017). Influence of water-borne epoxy resin content on performance of waterborne epoxy resin compound SBR modified emulsified asphalt for tack coat. *Construction and Building Materials*, 153, 774–782. doi:10.1016/j.conbuildmat.2017.07.148.
- [16] Wei, F., Cao, J., Zhao, H., & Han, B. (2021). Laboratory Investigation on the Interface Bonding between Portland Cement Concrete Pavement and Asphalt Overlay. *Mathematical Problems in Engineering*, 2021, 1–11. doi:10.1155/2021/8831287.
- [17] Ling, J., Wei, F., Zhao, H., Tian, Y., Han, B., & Chen, Z. (2019). Analysis of airfield composite pavement responses using full-scale accelerated pavement testing and finite element method. *Construction and Building Materials*, 212, 596–606. doi:10.1016/j.conbuildmat.2019.03.336.
- [18] Mateos, A., Harvey, J., Paniagua, J., Paniagua, F., & Liu, A. F. (2017). Mechanical characterisation of concrete-asphalt interface in bonded concrete overlays of asphalt pavements. *European Journal of Environmental and Civil Engineering*, 21, s43–s53. doi:10.1080/19648189.2017.1311808.
- [19] Leischner, S., Canon Falla, G., Gerowski, B., Rochlani, M., & Wellner, F. (2019). Mechanical Testing and Modeling of Interlayer Bonding in HMA Pavements. *Transportation Research Record*, 2673(11), 879–890. doi:10.1177/0361198119843254.
- [20] Mohod, M. V., & Kadam, K. N. (2016). A comparative study on rigid and flexible pavement: A review. *IOSR Journal of Mechanical and Civil Engineering (IOSR-JMCE)*, 13(3), 84–88.
- [21] Zhang, W. (2017). Effect of tack coat application on interlayer shear strength of asphalt pavement: A state-of-the-art review based on application in the United States. *International Journal of Pavement Research and Technology*, 10(5), 434–445. doi:10.1016/j.ijprt.2017.07.003.
- [22] Ali, M. H., Khalil, A. H., & Wang, Y. (2023). Experimental Study of the Effect of Tack Coats on Interlayer Bond Strength of Pavement. *Sustainability (Switzerland)*, 15(8), 6600. doi:10.3390/su15086600.
- [23] Kamal, I., & Bas, Y. (2021). Materials and technologies in road pavements - An overview. *Materials Today: Proceedings*, 42, 2660–2667. doi:10.1016/j.matpr.2020.12.643.
- [24] Haido, J. H., Tayeh, B. A., Majeed, S. S., & Karpuzcu, M. (2021). Effect of high temperature on the mechanical properties of basalt fibre self-compacting concrete as an overlay material. *Construction and Building Materials*, 268, 121725. doi:10.1016/j.conbuildmat.2020.121725.
- [25] Gao, F., Gao, X., Chen, Q., Li, Y., Gao, Z., & Wang, C. (2022). Materials and Performance of Asphalt-Based Waterproof Bonding Layers for Cement Concrete Bridge Decks: A Systematic Review. *Sustainability (Switzerland)*, 14(23), 15500. doi:10.3390/su142315500.
- [26] H., Wang, C., Niu, L., Yang, G., & Liu, L. (2022). Composition optimisation and performance evaluation of waterborne epoxy resin emulsified asphalt tack coat binder for pavement. *International Journal of Pavement Engineering*, 23(11), 4034–4048. doi:10.1080/10298436.2021.1932878.
- [27] Liu, L., Wang, C., & Liang, Q. (2022). Preparation of a heat insulation bonding layer for roads and its heat insulation effect. *Journal of Cleaner Production*, 365, 132828. doi:10.1016/j.jclepro.2022.132828.
- [28] DN-STR-03009. (2000). *Waterproofing and Surfacing of Concrete Bridge Decks*. TII Publications, Dublin, Ireland.
- [29] BBA-HAPAS. (2012). *Guidelines Document for the Assessment and Certification of Waterproofing Systems for Use on Concrete Decks of Highway Bridges*. British Board of Agrément (BBA), Watford, United Kingdom.
- [30] Russell, H. G. (2012). *Waterproofing membranes for concrete bridge decks*. Transportation Research Board, Washington, United States.
- [31] Khan, Z. A., Al-Abdul Wahab, H. I., Asi, I., & Ramadhan, R. (1998). Comparative study of asphalt concrete laboratory compaction methods to simulate field compaction. *Construction and Building Materials*, 12(6–7), 373–384. doi:10.1016/S0950-0618(98)00015-4.
- [32] Zhao, X., Niu, D., Zhang, P., Niu, Y., Xia, H., & Liu, P. (2022). Macro-meso multiscale analysis of asphalt concrete in different laboratory compaction methods and field compaction. *Construction and Building Materials*, 361, 129607. doi:10.1016/j.conbuildmat.2022.129607.
- [33] Shabani, R., Sengun, E., Ozturk, H. I., Alam, B., & Yaman, I. O. (2021). Superpave Gyrotory Compactor as an Alternative Design Method for Roller Compacted Concrete in the Laboratory. *Journal of Materials in Civil Engineering*, 33(6), 4021101. doi:10.1061/(asce)mt.1943-5533.0003714.
- [34] Wang, X., Ren, J., Hu, X., Gu, X., & Li, N. (2021). Determining Optimum Number of Gyrotations for Porous Asphalt Mixtures

- Using Superpave Gyratory Compactor. *KSCE Journal of Civil Engineering*, 25(6), 2010–2019. doi:10.1007/s12205-021-1005-x.
- [35] Xu, J., Li, N., & Xu, T. (2022). Temperature Changes of Interlaminar Bonding Layer in Different Seasons and Effects on Mechanical Properties of Asphalt Pavement. *International Journal of Pavement Research and Technology*, 15(3), 589–605. doi:10.1007/s42947-021-00039-9.
- [36] Zhang, H., Gao, P., Zhang, Z., & Pan, Y. (2020). Experimental study of the performance of a stress-absorbing waterproof layer for use in asphalt pavements on bridge decks. *Construction and Building Materials*, 254, 119290. doi:10.1016/j.conbuildmat.2020.119290.
- [37] Correia, N. S., Souza, T. R., Silva, M. P. S., & Kumar, V. V. (2023). Investigations on interlayer shear strength characteristics of geosynthetic-reinforced asphalt overlay sections at Salvador International Airport. *Road Materials and Pavement Design*, 24(6), 1542–1558. doi:10.1080/14680629.2022.2092021.
- [38] Lung, C. K., Mohd Hasan, M. R., Hamzah, M. O., Sani, A., Poovaneshvaran, S., & Ramadhansyah, P. J. (2020). Effect of temperatures and loading rates on direct shear strength of asphaltic concrete using layer-parallel direct shear test. *IOP Conference Series: Materials Science and Engineering*, 712(1), 12047. doi:10.1088/1757-899X/712/1/012047.
- [39] Vrtis, M., Rodezno, C., West, R., Podolsky, J., Calvert, J., & Van Deusen, D. (2023). NCAT Report 23-03, National Center for Asphalt Technology, Auburn University, Auburn, United States.
- [40] Recasens, R., Martínez, A., & Jiménez, F. (2006). Evaluation of Effect of Heat-Adhesive Emulsions for Tack Coats with Shear Test: From the Road Research Laboratory of Barcelona. *Transportation Research Record: Journal of the Transportation Research Board*, 1970, 64–70. doi:10.3141/1970-08.
- [41] Montgomery, D. C. (2017). *Design and analysis of experiments*. John Wiley & Sons, Hoboken, United States.